Longitudinal and Transverse Current Distributions on Microstriplines and Their Closed-Form Expression

MASANORI KOBAYASHI, MEMBER, IEEE

Abstract —Simple but accurate closed-form expressions for the normalized longitudinal and transverse current distributions on microstriplines are derived by using the charge conservation formula and the charge distributions calculated by the Green's function technique. Their dependence on both the relative permittivity of the substrate ϵ^* and the shape ratio w/h are explained, and the results are compared with other available results. It is confirmed by comparison with other theoretical results that the present closed-form expressions are valid for an even higher frequency. The reasonable expression for the normalized transverse current distribution is believed to be the first.

I. Introduction

IN THE MICROSTRIPLINE shown in Fig. 1, the electromagnetic fields can be obtained by the quasi-TEM mode analysis at low frequencies. The longitudinal current distribution $i_z(x)$, which is the source determining $\mathbb{H}$ for the case of the total longitudinal current $I(=Qv(f))\exp(-j\beta(f)z)$, can be approximated using the charge distribution $\sigma_0(x)$ on the strip of the microstripline without substrate ($\epsilon^*=1$) for a given total charge per unit length $Q/\epsilon^*_{\text{eff}}(0)$. We know the following approximate relation [1]:

$$i_z(x)=\epsilon^*_{\text{eff}}(0)\sigma_0(x)v(f)e^{-j\beta(f)z} \tag{1}$$

where $\epsilon^*_{\text{eff}}(0)$ denotes the effective relative permittivity at the frequency $f=0$, $\beta(f)$ the phase constant $(=\omega/v(f)$, $\omega=2\pi f)$, $v(f)\,(=v_0/\sqrt{\epsilon^*_{\text{eff}}(f)}\,)$ the phase velocity, $\epsilon^*_{\text{eff}}(f)$ the effective relative permittivity at the frequency f, and v_0 the velocity of light in free space. On the other hand, $\mathbb{E}$ can be approximated by the electrostatic field due to the charge distribution $\sigma(x)$ on the strip for a given total charge per unit length Q. However, we can find the following result [1]:

$$\sigma(x)\neq\epsilon^*_{\text{eff}}(0)\sigma_0(x) \tag{2}$$

except for the case of $\epsilon^*=1$.

Noticing this discrepancy, Denlinger [1] used the continuity equation for the time dependence $\exp(j\omega t)$

$$\frac{\partial i_x}{\partial x}+\frac{\partial i_z}{\partial z}=-j\omega\sigma(x)e^{-j\beta(f)z} \tag{3}$$

Manuscript received January 10, 1985; revised April 30, 1985.
The author is with the Department of Electrical Engineering, Faculty of Engineering, Ibaraki University, Hitachi, Ibaraki, Japan.

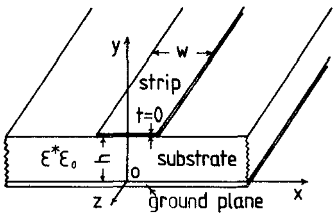

Fig. 1. Microstrip configuration.

and derived the following expression for obtaining the transverse current distribution on the strip:

$$i_x(x)=-j\omega(\operatorname{sgn}x)\int_0^x\{\sigma(x)-\epsilon^*_{\text{eff}}(0)\sigma_0(x)\}\,dx\,e^{-j\beta(f)z} \tag{4}$$

where

$$\operatorname{sgn}x=\begin{cases}-1, & x<0\\ +1, & x>0\end{cases}.$$

This idea is important because the accurate knowledge of not only $i_z(x)$ but also $i_x(x)$ is useful for calculating accurately the dispersion characteristics of the microstripline by the hybrid-mode analysis.

Itoh and Mittra [2], [3] proposed the spectral-domain analysis with powerful features. This dispersion analysis was studied by various workers and by various methods (see [4]–[11] and references therein). Kuester and Chang compared these many results, found significant discrepancies between them [4], and pointed out the validity of representing the current and charge distributions (especially the edge singularities) accurately with a minimum number of basis functions for use in various applications, such as determining radiation or mode fields of the lines, or frequency dispersion of the fundamental mode [5], [6]. In the spectral-domain analysis, the choice of the basis functions is important for numerical efficiency. If the first few basis functions approximate the actual unknown current reasonably well, the necessary size of the matrix can be held small for a given accuracy of the solution so that computation time is to be saved [3]. These closed-form expressions were given by Denlinger [1] and recently by Kuester and Chang [5]. The theoretical results were shown in [7]–[11].

In this paper, the charge distributions $\sigma(x)$ and $\sigma_0(x)$ are calculated with a high degree of accuracy by using the

0018-9480/85/0900-0784$01.00 ©1985 IEEE

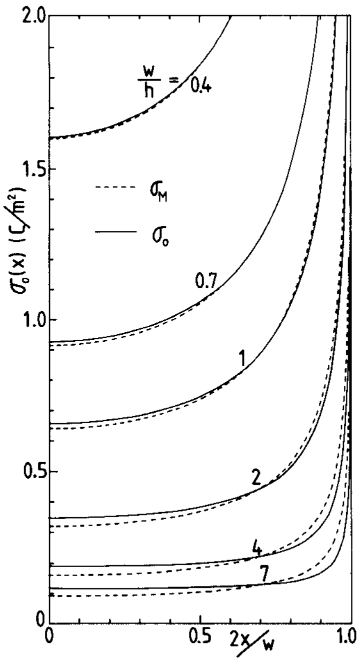

Fig. 2. Charge distributions on microstrip without substrate. Total charge on the strip is $Q = 1$. —— Exact results by the Green's function technique $\sigma_0(x)$. ---- Maxwell's distribution (5) $\sigma_M(x)$.

Green's function technique [13] for various cases with $\epsilon^* = 2, 4, 8, 16$, and $0.1 \leqslant w/h \leqslant 100$, and are used to calculate $i_z(x)$ and $i_x(x)$. The characteristics $i_z(x)$ versus w/h and also $i_x(x)$ versus ϵ^* and w/h are investigated in detail. Using these results, accurate closed-form expressions are given for the normalized longitudinal and transverse current distributions. The closed-form expression of the normalized transverse current distribution for the wide range of ϵ^* and w/h is believed to be the first.

II. Characteristics of $\sigma_0(x)$ Versus w/h

The charge distributions $\sigma_0(x)$ are the important quantities for determining the longitudinal and transverse current distributions, $i_z(x)$ in (1) and $i_x(x)$ in (4). The $\sigma_0(x)$ were calculated by the Green's function technique [9] for the various cases of the total charge $Q = 1$ on the strip in the microstripline without substrate in Fig. 1. Fig. 2 shows the comparison of these results $\sigma_0(x)$ and Maxwell's distribution $\sigma_M(x)$

$$\sigma_M(x) = \frac{2}{\pi w} \frac{1}{\sqrt{1 - \left(\frac{2x}{w}\right)^2}}. \tag{5}$$

We can find that the discrepancy of $\sigma_0(x)$ and $\sigma_M(x)$ becomes larger as w/h becomes larger because $\sigma_M(x)$ is the distribution for the case without a ground plane. However, the ratio $\sigma_0(0)/\sigma_M(0)$ at $x = 0$ approaches a constant value when $w/h \to \infty$. This value is $\pi/2$ because $\sigma_0(0) \to 1/w$ when $w/h \to \infty$. Fig. 3 shows the dependence of $\sigma_0(0)/\sigma_M(0)$ versus w/h. Fig. 4 shows the dependence of $\sigma_0(x)/\sigma_0(0)$ versus w/h to get the closed-form expression of $i_z(x)/i_z(0)$. The results of $\sigma_0(x)/\sigma_0(0)$ for the cases of $w/h \leqslant 0.7$ cannot be distinguished from each other in Fig. 4. Maxwell's distributions $\sigma_M(x)/\sigma_M(0)$ remains the same curve for all different w/h and also cannot be distinguished from the curves of $\sigma_0(x)/\sigma_0(0)$ for the cases of $w/h \leqslant 0.7$ in Fig. 4. Also, it seems that the curves of $\sigma_0(x)/\sigma_0(0)$ are obtained by pulling down the curve of $\sigma_M(x)/\sigma_M(0)$. Note the intersection point of the convex part of the curve $\sigma_0(x)/\sigma_0(0)$ for the arbitrary w/h and the straight line with the gradient angle of -45 degrees by $2x_c/w$ in Fig. 4. The closed-form expression of $\sigma_0(x)/\sigma_0(0)$ $(= i_z(x)/i_z(0))$ can be derived by pulling down the curve of $\sigma_M(x)/\sigma_M(0)$ with keeping $\sigma_M(x)/\sigma_M(0) = 1$ at $x = 0$ until its height at $x = x_c$ equals $\sigma_0(x_c)/\sigma_0(0)$. This process is also shown for the case $w/h = 4$ in Fig. 4. Fig. 5 shows the dependence of $2x_c/w$ versus w/h. The closed-form expression for $i_z(x)/i_z(0)$ $(= \sigma_0(x)/\sigma_0(0))$ obtained by this process is expressed as follows:

$$\frac{i_z(x)}{i_z(0)} = \frac{\sigma_0(x)}{\sigma_0(0)} = 1 + 10\left(1 - \frac{2x_c}{w}\right)\frac{M(x) - 1}{M(x_c) - 1} \tag{6}$$

where

$$M(x) = 1 \Big/ \sqrt{1 - (2x/w)^2}. \tag{7}$$

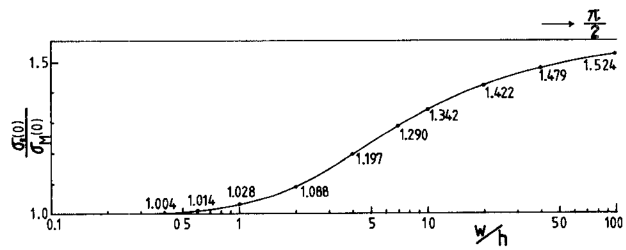

Fig. 3. Dependence of $\sigma_0(0)/\sigma_M(0)$ versus w/h.

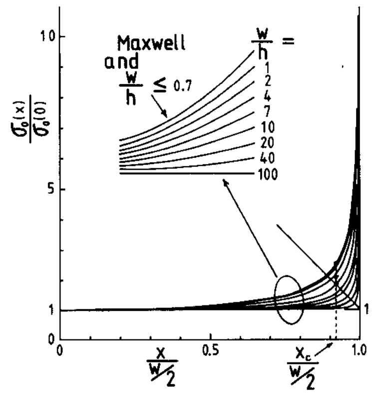

Fig. 4. Dependence of $\sigma_0(x)/\sigma_0(0)$ $(= i_z(x)/i_z(0))$ versus w/h. Maxwell's distributions $\sigma_M(x)/\sigma_M(0)$ remains the same curve for all different w/h and cannot be distinguished from $\sigma_0(x)/\sigma_0(0)$ for $w/h \leqslant 0.7$.

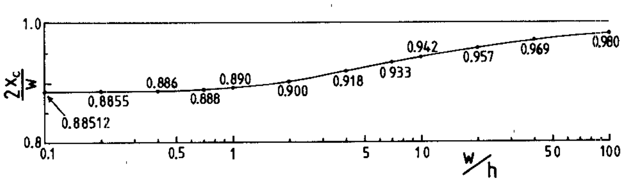

Fig. 5. Dependence of $2x_c/w$ versus w/h. $2x_c/w \to 0.88512$ when $w/h \to 0$ and $2x_c/w \to 1$ when $w/h \to \infty$.

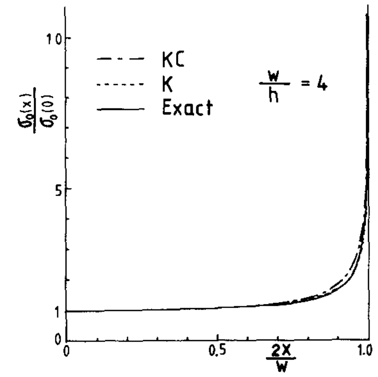

Fig. 6. Comparison of normalized charge distributions $\sigma_0(x)/\sigma_0(0)$ (= normalized longitudinal current distributions $i_z(x)/i_z(0)$). --- Kuester and Chang [5] (8). ---- Present expression (6). —— Exact result by the Green's function technique.

TABLE I
PERCENTAGE ERROR OF TWO CLOSED-FORM EXPRESSIONS OF $\sigma_0(x)/\sigma_0(0)$ ($= i_z(x)/i_z(0)$) WITH RESPECT TO THE EXACT RESULTS CALCULATED BY THE GREEN'S FUNCTION TECHNIQUE

2x/w \ w/h	0.7		1		2		4		7		10	
	KC	K	KC	K	KC	K	KC	K	KC	K	KC	K
0.330	0.2	0.1	0.4	0.2	1.0	0.7	0.9	1.2	-0.4	1.0	-0.8	0.8
0.488	0.4	0.1	0.8	0.4	2.1	1.3	2.1	2.4	-0.4	2.3	-1.5	1.9
0.657	0.8	0.5	1.4	0.6	3.8	1.9	4.3	3.8	0.5	4.3	-2.1	3.7
0.784	1.1	0.4	2.0	0.5	5.4	1.8	6.8	4.0	2.5	5.5	-1.2	5.4
0.875	1.4	-0.2	2.6	0.3	6.7	0.9	9.2	2.2	5.1	4.3	1.3	5.1
0.936	1.7	-0.4	3.0	-0.2	7.7	-0.7	11.0	-1.5	7.7	-0.4	4.1	0.8
0.973	2.0	-0.6	3.4	-0.6	8.5	-2.6	12.4	-6.5	9.6	-9.0	6.5	-8.0
0.992	2.6	-0.5	4.0	-0.8	9.4	-4.3	13.6	-11.7	11.1	-16.6	8.4	-19.1

KC : Kuester and Chang[5] K : present expression(6)

This closed-form expression satisfies the edge singularity [12] which requires that $i_z(x)$ approaches the edge $w/2$ of a strip with the singularity $|x-(w/2)|^{-1/2}$. Fig. 6 shows the comparison of the present expression (formula K) shown in (6) and the expression (formula KC) by Kuester and Chang [5]

$$\frac{\sigma_0(x)}{\sigma_0(0)} = \frac{\sqrt{\cosh^2\left(\frac{\pi w}{4h}\right)-1}}{\sqrt{\cosh^2\left(\frac{\pi w}{4h}\right)-\cosh^2\left(\frac{\pi x}{2h}\right)}}. \tag{8}$$

Table I shows the percentage error of these two formulas with respect to the exact results calculated by the Green's function technique [13]. We can find that formula K is the more closed-form for $w/h < 7$ and formula KC for $w/h > 7$. Fig. 7 shows the percentage error of the total charge by formula K with respect to the exact total charge. Its percentage error is less than -0.4 percent. The high degree of accuracy of formula K can be understood also by taking account of its agreement with the exact value at $x = x_c$.

The theoretical results for $i_z(x)$ were shown in the literature, for example, for the cases of $f = 1$ GHz in [7, fig. 4] and [9, fig. 6], $f = 10$ GHz in [8, fig. 6], $f = 12$ GHz in [11, fig. 5], and hk_0 ($k_0 = 2\pi/\lambda_0$) $= 0.01, 0.13$ in [10, figs. 13–15]. Comparing the results of the two formulas (K, KC) with these theoretical results, we can know that two formulas for $i_z(x)/i_z(0)$ are valid for even the higher frequency.

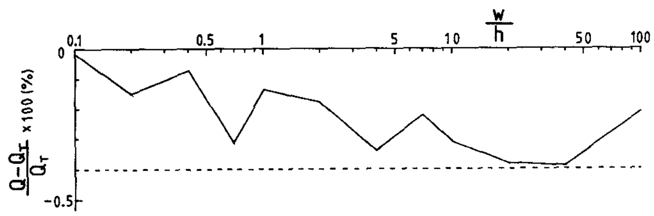

Fig. 7. Percentage error of the total charge by the present expression with respect to the exact total charge. Q_T = exact total charge by the Green's function technique, Q = total charge by the present expression (6).

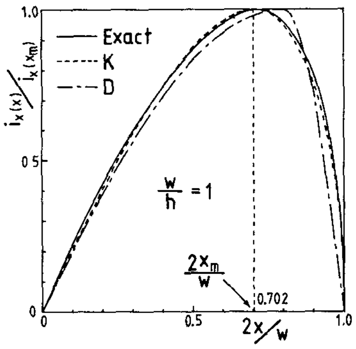

Fig. 8. Comparison of normalized longitudinal current distributions $i_x(x)/i_x(x_m)$ for $w/h = 1$. ---- Present expression (9) with $\alpha = 1.6$. --- Denlinger [1] (12). —— Exact result by the Green's function technique (not distinguished the curves for the cases of $\epsilon^* = 2,4,8,16$).

III. CHARACTERISTICS OF $i_x(x)$ VERSUS ϵ^* AND w/h

The current distribution $i_x(x)/i_x(x_m)$ normalized by $i_x(x_m)$ at the peak point $x = x_m$ can be calculated by substituting only the charge distributions $\sigma_0(x)$ and $\sigma(x)$ and the effective relative permittivity $\epsilon^*_{\text{eff}}(0)$ at the frequency $f = 0$ into (4). Here, $\sigma(x)$ denotes the charge distribution on the strip for the case with substrate for a total charge per unit length on the strip Q. On the other hand, $\sigma_0(x)$ denotes the charge distribution on the strip for the case without substrate for a total charge $Q/\epsilon^*_{\text{eff}}(0)$. The quantities $\sigma_0(x)$, $\sigma(x)$, and $\epsilon^*_{\text{eff}}(0)$ were obtained by the Green's function technique [13].

Fig. 8 shows the results of $i_x(x)/i_x(x_m)$ for the cases of $w/h = 1$ and $\epsilon^* = 2,4,8,16$ by the solid lines. For the case of $w/h = 40$, the results are similarly shown by the solid lines in Fig. 9. We cannot distinguish the curves for the cases of different ϵ^* in Figs. 8 and 9, and therefore can conclude that the dependence of $i_x(x)/i_x(x_m)$ versus ϵ^* is extremely small. This property is held for the cases of other w/h. This seems to be due to the small dependence of the effective filling fraction q versus ϵ^* [13, table I and fig. 8].

On the other hand, the dependence of $i_x(x)/i_x(x_m)$ versus w/h can be explained by the shift of the positions ($2x_m/w$) at those peak points. Fig. 10 shows the dependence of $2x_m/w$ versus w/h. The curve is obtained by taking the arithmetic mean of the results for the cases of $\epsilon^* = 2,4,8,16$. The percentage error of its value for the case of arbitrary ϵ^* versus the arithmetic mean value (Fig. 10) was less than ± 0.4 percent. It is worthwhile to say that the

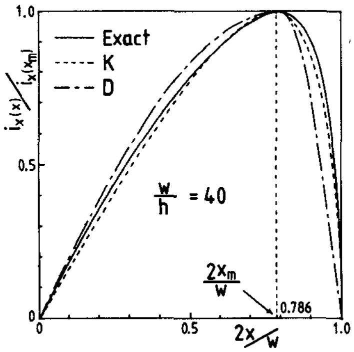

Fig. 9. Comparison of normalized longitudinal current distributions $i_x(x)/i_x(x_m)$ for $w/h = 40$. ---- Present expression (9) with $\alpha = 1.5$. --- Denlinger [1] (12). —— Exact result by the Green's function technique (not distinguished the curves for the cases of $\epsilon^* = 2,4,8,16$).

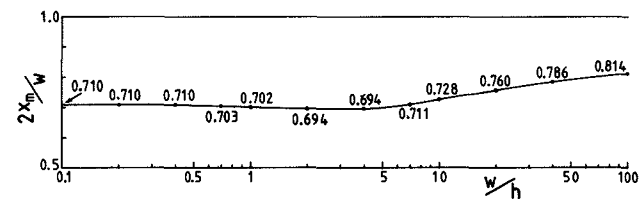

Fig. 10. Positions ($2x_m/w$) at the peak points of longitudinal current distributions versus w/h.

minimum part of this curve (Fig. 10) becomes nearly the inflection point of the curve of q versus w/h obtained by drawing the results shown in [13, table I].

We can derive the closed-form expression for $i_x(x)/i_x(x_m)$ to approximate the calculated results as follows:

$$\frac{i_x(x)}{i_x(x_m)} = \begin{cases} 1-\left(1-\dfrac{x}{x_m}\right)^{\alpha}, & 0 \leqslant x \leqslant x_m \\ \sqrt{1-\left(\dfrac{x-x_m}{\dfrac{w}{2}-x_m}\right)^2}, & x_m \leqslant x \leqslant \dfrac{w}{2} \end{cases} \tag{9}$$

$$i_x(-x) = -i_x(x) \tag{10}$$

where

$$\alpha = \begin{cases} 1.6, & \dfrac{w}{h} < 7 \\ 1.5, & 7 \leqslant \dfrac{w}{h}. \end{cases} \tag{11}$$

This closed-form expression satisfies the edge singularity [12] which requires that $i_x(x)$ behave like $|x-(w/2)|^{1/2}$ near the edge $w/2$ of a strip. Figs. 8 and 9 also show the comparison of the present expression (formula K) and the expression (formula D) by Denlinger [1, the correction is needed by $0.7 \rightarrow 0.8$ in (6)]

$$\frac{i_x(x)}{i_x\left(\dfrac{0.8w}{2}\right)} = \begin{cases} \sin\dfrac{\pi x}{0.8w}, & 0 \leqslant x \leqslant 0.8\dfrac{w}{2} \\ \cos\dfrac{\pi x}{0.2w}, & 0.8\dfrac{w}{2} \leqslant x \leqslant \dfrac{w}{2} \end{cases}. \tag{12}$$

In the spectral-domain analysis [2], [3], the phase constant $\beta(f)$ can be obtained from the determinant for the unknown amplitudes of $i_z(x)$ and $i_x(x)$ in the integral simultaneous equations. Therefore, its analysis needs the simple but accurate closed-form expressions of $i_z(x)/i_z(0)$ and $i_x(x)/i_x(x_m)$ to save computation time. The present expressions (6) and (9) satisfy the edge singularities [12] and are useful for its analysis with a minimum number of basis functions.

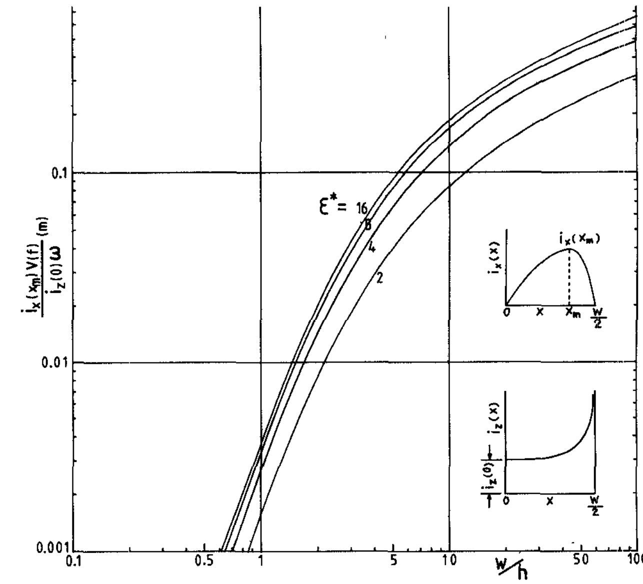

Fig. 11. Dependence of $i_x(x_m)v(f)/(i_z(0)\omega)$ obtained by the Green's function technique versus ϵ^* and w/h. The results are valid for the low-frequency region ($f \leqslant f_i/10$ [14]).

Fig. 11 shows the dependence of $i_x(x_m)v(f)/(i_z(0)\omega)$ versus ϵ^* and w/h. The results are valid for the low-frequency region where the quasi-TEM approximation can be applied. The expressions (1) and (4) are valid in this frequency region. For the microstripline, the quasi-TEM mode is dominant until the frequency $f = f_i/10$ [14], where f_i denotes the inflection frequency of the dispersion curve of $1/\sqrt{\epsilon^*_{\text{eff}}(f)}$. Therefore, within this frequency range, the ratio $i_x(x_m)/i_z(0)$ can be found with the help of Fig. 11.

However, the present closed-form expressions $i_z(x)/i_z(0)$ and $i_x(x)/i_x(x_m)$ are believed to be valid for even the higher frequency although no exact results can be referenced in the literature. It is worthwhile to say that the present expression of $i_x(x)/i_x(x_m)$ ($2x_m/w$ = about 0.702 for $w/h = 0.96$ and 0.74 for $w/h = 14.3$ in Fig. 10) has good agreement with the theoretical results by Fujiki *et al.* [7, $2x_m/w$ = about 0.7 for $w/h = 0.96$ in fig. 4] for the case of $\epsilon^* = 9.7$, $h = 1.27$ mm, $w = 1.219$ mm, $f = 1$ GHz, and by Jansen [11, $2x_m/w$ = about 0.72 for $w/h = 14.3$ in fig. 5] for the case of $\epsilon^* = 9.7$, $h = 0.64$ mm, $w = 9.15$ mm, $f = 12$ GHz.

IV. Conclusion

It has been shown that the normalized longitudinal and transverse current distributions of the microstriplines $i_z(x)/i_z(0)$ and $i_x(x)/i_x(x_m)$ are approximated quite well by (6) and (9) over the wide range of ϵ^* and w/h. The small dependence of $i_x(x)/i_x(x_m)$ versus ϵ^* has been explained by the small dependence of q versus ϵ^*. The reasonable expression for the normalized transverse current distribution is believed to be the first. The present closed-form expressions of $i_z(x)/i_z(0)$ and $i_x(x)/i_x(x_m)$ are naturally valid for the low-frequency range ($f \leqslant f_i/10$) where the quasi-TEM approximation can be applied. However, they are believed to be valid for even the higher frequency. This has been confirmed by comparing them with the other theoretical results shown for the higher frequency.

Using these current distributions, the dispersion characteristics of the microstriplines will be performed by using the spectral-domain analysis in the near future. Also, these closed-form expressions will be useful in many applications as shown by Kuester and Chang [5], [6].

References

[1] E. J. Denlinger, "A frequency dependent solution for microstrip transmission lines," *IEEE Trans. Microwave Theory Tech.*, vol. MTT-19, pp. 30–39, Jan. 1971.

[2] T. Itoh and R. Mittra, "Spectral-domain approach for calculating the dispersion characteristics of microstriplines," *IEEE Trans. Microwave Theory Tech.*, vol. MTT-21, pp. 496–499, July 1973.

[3] T. Itoh and R. Mittra, "A technique for computing dispersion characteristics of shielded microstriplines," *IEEE Trans. Microwave Theory Tech.*, vol. MTT-21, pp. 896–898, Oct. 1974.

[4] E. F. Kuester and D. C. Chang, "An appraisal of methods for computation of the dispersion characteristics of open microstrip," *IEEE Trans. Microwave Theory Tech.*, vol. MTT-27, pp. 691–694, July 1979.

[5] E. F. Kuester and D. C. Chang, "Closed-form expressions for the current or charge distribution on parallel strips or microstrips," *IEEE Trans. Microwave Theory Tech.*, vol. MTT-28, pp. 254–259, Mar. 1980.

[6] E. F. Kuester and D. C. Chang, "Theory of dispersion in microstrip of arbitrary width," *IEEE Trans. Microwave Theory Tech.*, vol. MTT-28, pp. 259–265, Mar. 1980.

[7] Y. Fujiki, Y. Hayashi, and M. Suzuki, "Analysis of strip transmission lines by iteration method," *J. Inst. Electron. Commun. Eng. Japan*, vol. 55-B, pp. 212–219, May 1972 (in Japanese); *Electron. Commun. Japan*, vol. 55, pp. 74–80, May 1972.

[8] J. C. Minor and D. M. Bolle, "Modes in the shielded microstrip on a ferrite substrate transversely magnetized in the plane of the substrate," *IEEE Trans. Microwave Theory Tech.*, vol. MTT-19, pp. 570–577, July 1971.

[9] D. T. Yeh and D. M. Bolle, "Characteristic impedance and field patterns of the shielded microstrip on a ferrite substrate," *IEEE Trans. Microwave Theory Tech.*, vol. MTT-23, pp. 585–588, July 1975.

[10] M. K. Krage and G. I. Haddad, "Frequency-dependent characteristics of microstrip transmission lines," *IEEE Trans. Microwave Theory Tech.*, vol. MTT-20, pp. 678–688, Oct. 1972.

[11] R. H. Jansen, "High-speed computation of single and coupled microstrip parameters including dispersion, high-order modes, loss and finite strip thickness," *IEEE Trans. Microwave Theory Tech.*, vol. MTT-26, pp. 75–82, Feb. 1978.

[12] R. Mittra and S. W. Lee, *Analytical Techniques in the Theory of Guided Waves*. New York: Macmillan, 1971, pp. 4–11.

[13] M. Kobayashi, "Analysis of the microstrip and the electrooptic light modulators," *IEEE Trans. Microwave Theory Tech.*, vol. MTT-26, pp. 119–126, Feb. 1978. Main misprints: $-\alpha \rightarrow -\alpha)$ in (31), $(1-K)^2 \rightarrow (1-K^2)$ in (33), $(\text{---})\nu \rightarrow (\text{---})^{\gamma}$ in (37), larger → smaller in right below Table III, $(\text{---})\nu \rightarrow (\text{---})^{\gamma}$ in (46), 2[μm] → 2[mm] in Table IV.

[14] M. Kobayashi, "Important role of inflection frequency in the dispersive property of microstriplines," *IEEE Trans. Microwave Theory Tech.*, vol. MTT-30, pp. 2057–2059, Nov. 1982.

Masanori Kobayashi (M'79) was born in Niigata, Japan, on June 17, 1947. He received the B.E. and M.E. degrees in electrical engineering from the Ibaraki University, Ibaraki, Japan, in 1970 and 1972, respectively, and the D.E. degree in electrical and electronic engineering from the Tokyo Institute of Technology, Tokyo, Japan, in 1981.

Since April 1972, he has been with the Department of Electrical Engineering, Ibaraki University. He was a Research Assistant from April 1972 to March 1981 and a Lecturer from April 1981 to July 1982. Since August 1982, he has been an Associate Professor. His research interests are in the areas of microstrip transmission lines, dielectric optical waveguides, magnetic elements, and relativistic electromagnetic theory.

Dr. Kobayashi is a member of the Institute of Electrical Engineers of Japan and the Institute of Electronics and Communication Engineers of Japan.